

## Original Articles

# Silicon Micromachining to Tissue Engineer Branched Vascular Channels for Liver Fabrication

SATOSHI KAIHARA, M.D.,<sup>1,3</sup> JEFFREY BORENSTEIN, Ph.D.,<sup>2,3</sup>  
RAHUL KOKA, B.A.,<sup>1,3</sup> SONAL LALAN, B.A.,<sup>1,3</sup> ERIN R. OCHOA, M.D.,<sup>3,4</sup>  
MICHAEL RAVENS,<sup>1,3</sup> HOMER PIEN, Ph.D.,<sup>2,3</sup> BRIAN CUNNINGHAM, Ph.D.,<sup>2,3</sup>  
and JOSEPH P. VACANTI, M.D.<sup>1,3</sup>

### ABSTRACT

To date, many approaches to engineering new tissue have emerged and they have all relied on vascularization from the host to provide permanent engraftment and mass transfer of oxygen and nutrients. Although this approach has been useful in many tissues, it has not been as successful in thick, complex tissues, particularly those comprising the large vital organs such as the liver, kidney, and heart. In this study, we report preliminary results using micromachining technologies on silicon and Pyrex surfaces to generate complete vascular systems that may be integrated with engineered tissue before implantation. Using standard photolithography techniques, trench patterns reminiscent of branched architecture of vascular and capillary networks were etched onto silicon and Pyrex surfaces to serve as templates. Hepatocytes and endothelial cells were cultured and subsequently lifted as single-cell monolayers from these two-dimensional molds. Both cell types were viable and proliferative on these surfaces. In addition, hepatocytes maintained albumin production. The lifted monolayers were then folded into compact three-dimensional tissues. Thus, with the use microfabrication technology in tissue engineering, it now seems feasible to consider lifting endothelial cells as branched vascular networks from two-dimensional templates that may ultimately be combined with layers of parenchymal tissue, such as hepatocytes, to form three-dimensional conformations of living vascularized tissue for implantation.

### INTRODUCTION

**T**HE FIELD OF TISSUE ENGINEERING is now maturing and undergoing explosive growth.<sup>1-4</sup> Virtually every tissue and organ of the body has been studied. Many tissue-engineering technologies are becoming

---

<sup>1</sup>Department of Surgery, Harvard Medical School and the Massachusetts General Hospital, Boston, Massachusetts.

<sup>2</sup>The Charles Stark Draper Laboratories, Cambridge, Massachusetts.

<sup>3</sup>The Center For Innovative Minimally Invasive Therapy, Boston, Massachusetts.

<sup>4</sup>Department of Pathology, Harvard Medical School and Massachusetts General Hospital, Boston, Massachusetts.

available for human use.<sup>5-13</sup> Over time, several techniques to engineer new living tissue have been studied. Technologies include the use of growth factors to stimulate wound repair and regeneration, techniques of guided tissue regeneration using nonliving matrices to guide new tissue development, cell transplantation, and cell transplantation on matrices.<sup>14</sup> More recently, new understanding in stem cell biology has led to studies of populations of primordial cells, stem cells, or embryonic stem cells to use in tissue engineering approaches.<sup>15,16</sup> To date, all approaches in tissue engineering have relied on the in-growth of blood vessels into tissue-engineered devices to achieve permanent vascularization. This strategy has worked well for many tissues. However, it falls short for thick, complex tissues such as large vital organs, including liver, kidney, and heart. Techniques using three-dimensional printing technology to achieve ordered arrays of channels have been described to begin to solve this problem.<sup>17,18</sup>

In parallel to these advances, the rapidly emerging field of MicroElectroMechanical Systems (MEMS) has penetrated a wide array of applications, in areas as diverse as automotives, inertial guidance and navigation, microoptics, chemical and biological sensing, and, most recently, biomedical engineering.<sup>19,20</sup> Microfabrication methods for MEMS represent an extension of semiconductor wafer process technology originally developed for the integrated circuit (IC) industry. Control of features down to the submicron level is routinely achieved in IC processing of electrical circuit elements; MEMS technology translates this level of control into mechanical structures at length scales stretching from  $<1 \mu\text{m}$  to  $>1 \text{cm}$ . Standard bulk micromachining enables patterns of arbitrary geometry to be imprinted into wafers using a series of subtractive etching methods. Three-dimensional structures can be realized by superposition of these process steps using precise alignment techniques.

Several groups have used these highly precise silicon arrays to control cell behavior and study gene expression and cell-surface interactions.<sup>21,22,23</sup> However, this approach is essentially a two-dimensional technology, and it has not been apparent that it might be adapted to the generation of thick, three-dimensional tissues. We now report early studies using microfabrication in silicon and Pyrex to generate hepatic tissue and vascular tissue that may be able to be combined to form thick, three-dimensional vascularized tissues.

## MATERIALS AND METHODS

### *Micromachining techniques*

Templates for the formation of sheets of living vascularized tissue were fabricated utilizing micromachining technology. For the present work, a single-level etch was used to transfer a vascular network pattern into an array of connected trenches in the surface of both silicon and Pyrex wafers.

In this prototype, a simple geometry was selected for patterning the vascular network. Near the edge of each wafer, a single inlet or outlet was positioned, with a width of  $500 \mu\text{m}$ . After a short length, the inlet and outlet branched into three smaller channels of width  $250 \mu\text{m}$ ; each of these branched again into three  $125\text{-}\mu\text{m}$  channels, and finally down to three  $50\text{-}\mu\text{m}$  channels. From the  $50\text{-}\mu\text{m}$  channels extends the capillary network, which comprises the bulk of the layout. In between these inlet and outlet networks lies a tiled pattern of diamonds and hexagons forming a capillary bed and filling the entire space between the inlet and outlet. In one configuration, the capillary width was set at  $25 \mu\text{m}$ , whereas the other capillaries were fixed at  $10 \mu\text{m}$ . This geometry was selected because of its simplicity as well as its rough approximation to the size scales of the branching architecture of the liver. Layout of this network was accomplished using CADENCE software (Cadence, Chelmsford, MA) on a Silicon Graphics workstation. A file with the layout was generated and sent electronically to Align-Rite (Burbank, California), where glass plates with electron beam-generated patterns replicating the layout geometry were produced and returned for lithographic processing.

Starting materials for tissue engineering template fabrication were standard semiconductor-grade silicon wafers (Virginia Semiconductor, Powhatan, Virginia), and standard Pyrex wafers (Bullen Ultrasonics, Eaton, Ohio) suitable for MEMS processing. Silicon wafers were  $100 \text{mm}$  in diameter and  $525 \mu\text{m}$  thick, with primary and secondary flats cut into the wafers to signal crystal orientation. Crystal orientation was  $<100>$ , and wafers were doped with boron to a resistivity of approximately  $5 \text{W-cm}$ . The front surface was polished to an optical finish and the back surface ground to a matte finish. Pyrex wafers were of composition

identical to Corning 7740 (Corning Glass Works, Corning NY), and were also 100 mm in diameter, but had a thickness of 775 microns. Both front and back surfaces were polished to an optical finish. Prior to micromachining, both wafer types were cleaned in a mixture of 1 part  $\text{H}_2\text{SO}_4$  to 1 part  $\text{H}_2\text{O}_2$  for 20 min at  $140^\circ\text{C}$ , rinsed eight times in deionized water with a resistivity of 18 MW, and dried in a stream of hot  $\text{N}_2$  gas.

For silicon and Pyrex wafers, standard photolithography was employed as the etch mask for trench formation. Etching of Pyrex wafers requires deposition of an intermediate layer for pattern transfer that is impervious to the etch chemistry. A layer of polysilicon of thickness  $0.65\ \mu\text{m}$  over the Pyrex was utilized for this purpose. This layer was deposited using Low Pressure Chemical Vapor Deposition (LPCVD) at  $570^\circ\text{C}$  and 500 mTorr via the standard silane decomposition method. In the case of silicon, photoresist alone could withstand limited exposure to two of the three etch chemistries employed. For the third chemistry, a  $1.0\text{-}\mu\text{m}$  layer of silicon dioxide was thermally deposited at  $1100^\circ\text{C}$  in hydrogen and oxygen.

Once the wafers were cleaned and prepared for processing, images of the prototype branching architecture were translated onto the wafer surfaces using standard MEMS lithographic techniques. A single layer of photoresist (Shipley 1822, MicroChem Corp., Newton, MA) was spun onto the wafer surfaces at 4000 rpm, providing a film thickness of approximately  $2.4\ \mu\text{m}$ . After baking at  $90^\circ\text{C}$  for 30 min, the layer of photoresist was exposed to UV light using a Karl Suss MA6 (Suss America, Waterbury, VT) mask aligner. Light was passed through the lithographic plate described earlier, which was in physical contact with the coated wafer. This method replicates the pattern on the plate to an accuracy of  $0.1\ \mu\text{m}$ . Following exposure, wafers were developed in Shipley 319 Developer (MicroChem Corp., Newton, MA), and rinsed and dried in deionized water. Finally, wafers were baked at  $110^\circ\text{C}$  for 30 min to harden the resist, and exposed to an oxygen plasma with 80 Watts of power for 42 s to remove traces of resist from open areas.

Silicon wafers were etched using three different chemistries, whereas Pyrex wafers were processed using only one technique. For Pyrex, the lithographic pattern applied to the polysilicon intermediate layer was transferred using a brief ( $\sim 1$  min) exposure to  $\text{SF}_6$  in a reactive ion-etching plasma system (Surface Technology Systems [STS] Newport, UK). Photoresist was removed, and the pattern imprinted into the polysilicon layer was transferred into trenches in the silicon using a mixture of two parts  $\text{HNO}_3$  to one part HF at room temperature. With an etch rate of 1.7 microns per minute, 20-micron-deep trenches were etched into the Pyrex wafers in approximately 12 min. Because the chemistry is isotropic, as the trenches are etched they become wider. Processing with the layout pattern with  $25\text{-}\mu\text{m}$ -wide capillary trenches tended to result in merging of the channels, while the use of  $10\text{-}\mu\text{m}$ -wide trenches avoided this phenomenon. Interferometric analysis of the channels after etching showed that surface roughness was less than  $0.25\ \mu\text{m}$ . Once channel etching of Pyrex wafers was completed, polysilicon was removed with a mixture of 10 parts  $\text{HNO}_3$  to one part HF at room temperature, and wafers were recleaned in one part  $\text{H}_2\text{SO}_4$  to one part HF.

Three different chemistries were employed to etch silicon and investigate the interaction between channel geometry and cell behavior. First, a standard anisotropic plasma etch chemistry, using a mixture of  $\text{SF}_6$  and  $\text{C}_4\text{F}_8$  in a switched process plasma system from STS,<sup>24</sup> was used to produce rectangular trenches in silicon. An example of this process is shown in Fig. 1; note that narrower trenches are shallower than deep trenches due to a phenomenon known as RIE lag. A second process utilized a different plasma system from STS, which produces isotropic trenches with a U-shaped profile, shown schematically in Fig. 2. Although the process is isotropic, widening of the trenches is not as severe as is experienced in the isotropic Pyrex etching process described earlier. In both of these plasma-etching cases, trenches were etched to a nominal depth of  $20\ \mu\text{m}$ . For the third process, anisotropic etching in KOH (45% wt/wt in  $\text{H}_2\text{O}$  at  $88^\circ\text{C}$ ), the intermediate silicon dioxide layer mentioned above was employed. First, the silicon dioxide layer was patterned using HF etching at room temperature. The KOH process produces angled sidewalls rather than the rectangular profile or U-shaped profile produced by the first two recipes, respectively. Crystal planes in the  $\langle 111 \rangle$  orientation are revealed along the angled sidewalls, due to anisotropic properties of the KOH etch process as a function of crystal orientation.<sup>25</sup> Due to the self-limiting nature of the channels produced by this process, trench depth was limited to  $10\ \mu\text{m}$ . After completion of the silicon wafer etching, all layers of photoresist and silicon dioxide were removed, and wafers were cleaned in one part  $\text{H}_2\text{SO}_4$  to one part  $\text{H}_2\text{O}_2$  at  $140^\circ\text{C}$ , followed by rinsing in deionized water and drying in nitrogen gas.

For this set of experiments, no attempt was made to alter the surface chemistry of the silicon and Pyrex

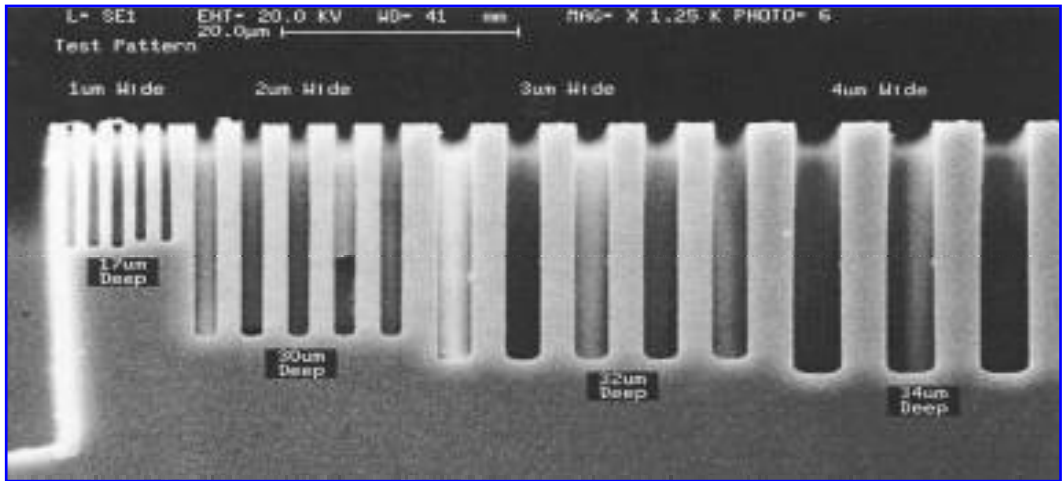


**FIG. 1.** Process for fabricating U-shaped trenches in silicon wafers.

wafers. Prior to processing, silicon wafers were uniformly hydrophobic, whereas Pyrex wafers were equally hydrophilic, as determined by observations of liquid sheeting and sessile drop formation. After processing, unetched surfaces appeared to retain these characteristics, but the surface chemistry within the channels was not determined.

### *Animals*

Adult male Lewis rats (Charles River Laboratories, Wilmington, MA), weighing 150–200 g, were used as cell donors. Animals were housed in the Animal Facility of Massachusetts General Hospital in accordance with National Institutes of Health (NIH) guide lines for the care of laboratory animals. They were allowed rat chow and water *ad libitum* and maintained in 12-h light and dark cycle.

### *Cell isolations*

Male Lewis rats were used as hepatic cell donors. Hepatocytes were isolated using a modified two-step collagenase perfusion procedure as described in previous reports.<sup>26,27</sup> Briefly, the animals were anesthetized with nembutal sodium solution (Abbott Laboratories, North Chicago, IL), 50 mg/kg, and the abdomen was prepared in sterile fashion. A midline abdominal incision was made and the infrahepatic inferior vena cava was cannulated with a 16-gauge angiocatheter (Becton Dickinson). The portal vein was incised to allow retrograde efflux and the suprahepatic inferior vena cava was ligated. The perfusion was performed at a

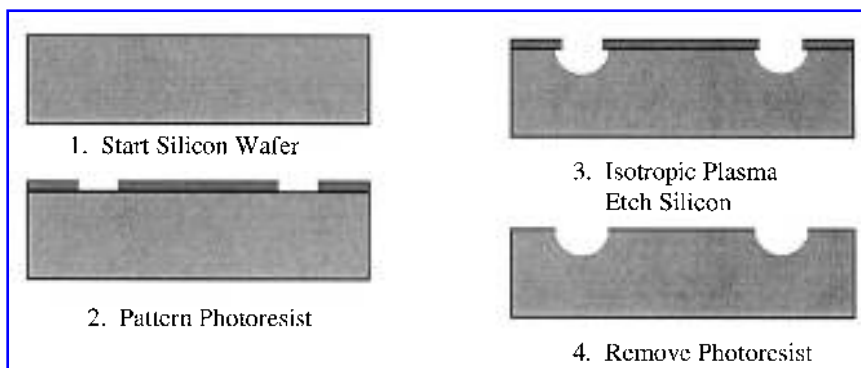


**FIG. 2.** Test structure pattern etched using inductively-couple d (IPC) system described in the text.

flow rate of 29 mL/min initially with a calcium-free buffer solution for 5–6 min, then with a buffer containing collagenase type 2 (Worthington Biomedical Corp., Freehold, NJ) at 37°C. The liver was excised after adequate digestion of the extracellular matrix and mechanically agitated in William's E medium (Sigma, St. Louis, MO) with supplements to produce a single-cell suspension. The suspension was filtered through a 300- $\mu$ m mesh and separated into two fractions by centrifugation at 50 g for 2 min at 4°C. The pellet containing the viable hepatocyte fraction was resuspended in William's E medium and further purified by an isodensity Percoll centrifugation. The resulting pellet was then resuspended in hepatocyte growth medium, and cell counts and viabilities of HCs were determined using the trypan blue exclusion test.

The endothelial cells were derived from rat lung microvessels and they were purchased directly from the vendor (Vascular Endothelial Cell Technologies, Rensselaer, NY).

#### *Hepatocyte culture medium*

William's E medium supplemented with 1g of sodium pyruvate (Sigma, St. Louis, MO) and 1% glutamine-penicillin-streptomycin (Gibco BRL, Gaithersburg, MD) were used during the cell isolation process. The plating medium was Dulbecco's modified Eagle medium (DMEM; Gibco BRL) supplemented with 10% fetal bovine serum (FBS), 1% penicillin-streptomycin, 44 mM sodium-bicarbonate, 20 mM HEPES, 10 mM niacinamide, 30  $\mu$ g/mL L-proline, 1 mM ascorbic acid-2-phosphate, 0.1  $\mu$ M dexamethasone (Sigma), insulin-transferrin-sodium selenite (5 mg/L-5  $\mu$ g/L, Roche Molecular Biomedicals, Indianapolis, IN), and 20 ng/mL epidermal growth factor (Collaborative Biomedical Products, Bedford, MA).

#### *Endothelial cell culture medium*

We used a modified version of a previously used endothelial cell culture medium.<sup>28</sup> DMEM (Gibco BRL) was supplemented with 10% FBS, 1% penicillin-streptomycin, 25 mg of ascorbic acid (Sigma), 10 mg of L-alanine (Sigma), 25 mg of L-proline (Sigma), 1.5  $\mu$ g of cupric sulfate (Sigma), glycine (Sigma), and 1 M HEPES buffer solution (Gibco BRL). The media was supplemented with 8 mg of ascorbic acid every day.

#### *Cell attachment and lifting from nonetched silicon and Pyrex wafers*

Silicon and Pyrex were both tested as possible substrates for the culture and lifting of endothelial cells and hepatocytes. Prior to cell seeding, the Pyrex wafers were sterilized with 70% ethanol (Fisher, Pittsburg, PA) overnight and washed three times with sterile phosphate-buffered saline (PBS; Gibco BRL). Silicon wafers were first soaked in acetone for 1 h, followed a methanol rinse for 15 min, and overnight sterilization in 100% isopropyl alcohol. Rat lung microvascular endothelial cells was cultured on noncoated Pyrex and silicon surfaces, as well as wafers coated with vitrogen (30  $\mu$ g/mL), Matrigel® (1%), or Gelatin (10 mg/mL). Once isolated, the cells were resuspended in endothelial cell culture medium, seeded uniformly onto the wafer at a density of  $26.7 \times 10^3$  cells/cm<sup>2</sup> and cultured at 5% CO<sub>2</sub> and 37°C. After reaching confluence, we tested the ability for the monolayer of endothelial cells to lift from the wafers using a cell scraper to promote detachment.

The rat hepatocytes were also cultured on noncoated Pyrex and silicon, as well as wafers coated with a thin and thick layers of vitrogen (30  $\mu$ g/mL and 3  $\mu$ g/mL) and Matrigel (1%) to determine the optimal methods for lifting hepatocyte sheets. Once isolated, the hepatocytes were resuspended in hepatocyte growth media, seeded onto the wafer at a density of  $111.3 \times 10^3$  cells/cm<sup>2</sup>, and cultured at 5% CO<sub>2</sub> and 37°C. Cell attachment and growth was observed daily using microscopy and cell lifting occurred spontaneously.

After determining which method for culturing was best for lifting the hepatocytes and endothelial cells in an intact layer, both membranes were fixed in 10% buffered formalin for 1 h and harvested for histological study. The hepatocytes were stained immunohistochemically.

#### *Immunohistochemical staining*

The hepatocyte cell monolayer membrane was fixed in 10% buffered formalin and processed for hematoxylin-eosin and immunohistochemical staining using a labeled streptavidin biotin method (LSAB2 kit for rat specimen, DAKO, Carpinteria, CA). The primary antibody was rabbit anti-albumin (ICN, Costa Mesa,

CA). Three-micron sections were prepared and deparaffinized. The specimens were treated with peroxidase blocking buffer (DAKO) to prevent the nonspecific staining. Sections were stained with albumin diluted with PBS, followed by biotinylated anti-rabbit antibody and horseradish peroxidase (HRP)-conjugated streptavidin. Sections were treated with diaminobenzidine (DAB) as substrate and were counterstained with hematoxylin.

### *Albumin production*

To assess hepatocyte function, albumin concentration in the culture medium was measured every 24 h for 5 days pre-cell detachment using an enzyme-linked immunosorbent assay (ELISA) ( $n = 5$ ).<sup>29</sup> In brief, a 96-well microplate was coated with anti-rat albumin antibody (ICN). After blocking nonspecific responses with a 1% gelatin solution, each sample was seeded onto the plate and incubated for 1 h. This was followed by another 1-h incubation with peroxidase conjugated anti-rat albumin antibody (ICN). Finally, the substrate was added and extinction was measured with a microplate reader at 410 nm.  $R^2$  of the standard curve was  $>0.99$ .

### *Statistical analysis*

All data were expressed as mean  $\pm$  SD. Statistical analysis was performed with a paired  $t$ -test. When the  $p$  value of each test was less than 0.05, we judged it to be statistically significant.

### *Cell attachment to etched silicon and Pyrex wafers*

Endothelial cells and hepatocytes were also seeded onto etched silicon and Pyrex wafers. Prior to cell seeding, the Pyrex wafers were sterilized with 70% ethanol (Fisher) overnight and washed three times with sterile PBS (Gibco BRL). Silicon wafers were first soaked in acetone for 1 h, followed a methanol rinse for 15 min, and overnight sterilization in 100% isopropyl alcohol. Onto these wafers were seeded rat lung microvascular endothelial cells at a density of  $26.7 \times 10^3$  cells/cm<sup>2</sup>, or rat hepatocytes at a density of  $111.3 \times 10^3$  cells/cm<sup>2</sup>. These cells were cultured at 5% CO<sub>2</sub> and 37°C, and their attachment and growth observed daily using microscopy.

### *Implantation of hepatocyte sheets into the rat omentum*

Hepatocytes were cultured on silicon wafers coated with a thin layer of vitrogen (30  $\mu$ g/ml), and lifted in sheets. Retrorsine is a drug known to inhibit the regeneration of the normal liver by producing a block in the hepatocyte cell cycle with an accumulation of cells in late S and/or G<sub>2</sub> phase.<sup>30</sup> This drug was administered into the peritoneal cavity of two rats at a dose of 3 mg/mL per 100 g on day 0, and after 2 weeks. Three weeks later, a portacaval shunt was created, and the following week a hepatocyte sheet, lifted after 4 days culture on vitrogen-coated silicon (30  $\mu$ g/mL), was implanted onto the microvasculature of the rat omentum and rolled into a three-dimensional cylinder, and a 60% hepatectomy was performed. The rolled omentum with hepatocytes was harvested at 4 weeks and at 3 months after implantation and analyzed using histology.

## RESULTS

### *Micromachining*

A schematic of the vascular branching network design used as a template for micromachining is shown in Fig. 3A. This pattern was transferred to silicon and Pyrex wafers using the processes described in the Materials and Methods section. Typical trench depths of 20 microns on silicon and 10 microns on glass were achieved utilizing these processes. An optical micrograph of a portion of the capillary network etched into a silicon wafer is shown in Fig. 3B. In Fig. 3C, a scanning electron micrograph cross section of an angled trench etched using the anisotropic etching process described earlier is shown. This process resulted in excellent adhesion and enhanced lifting of living tissue.

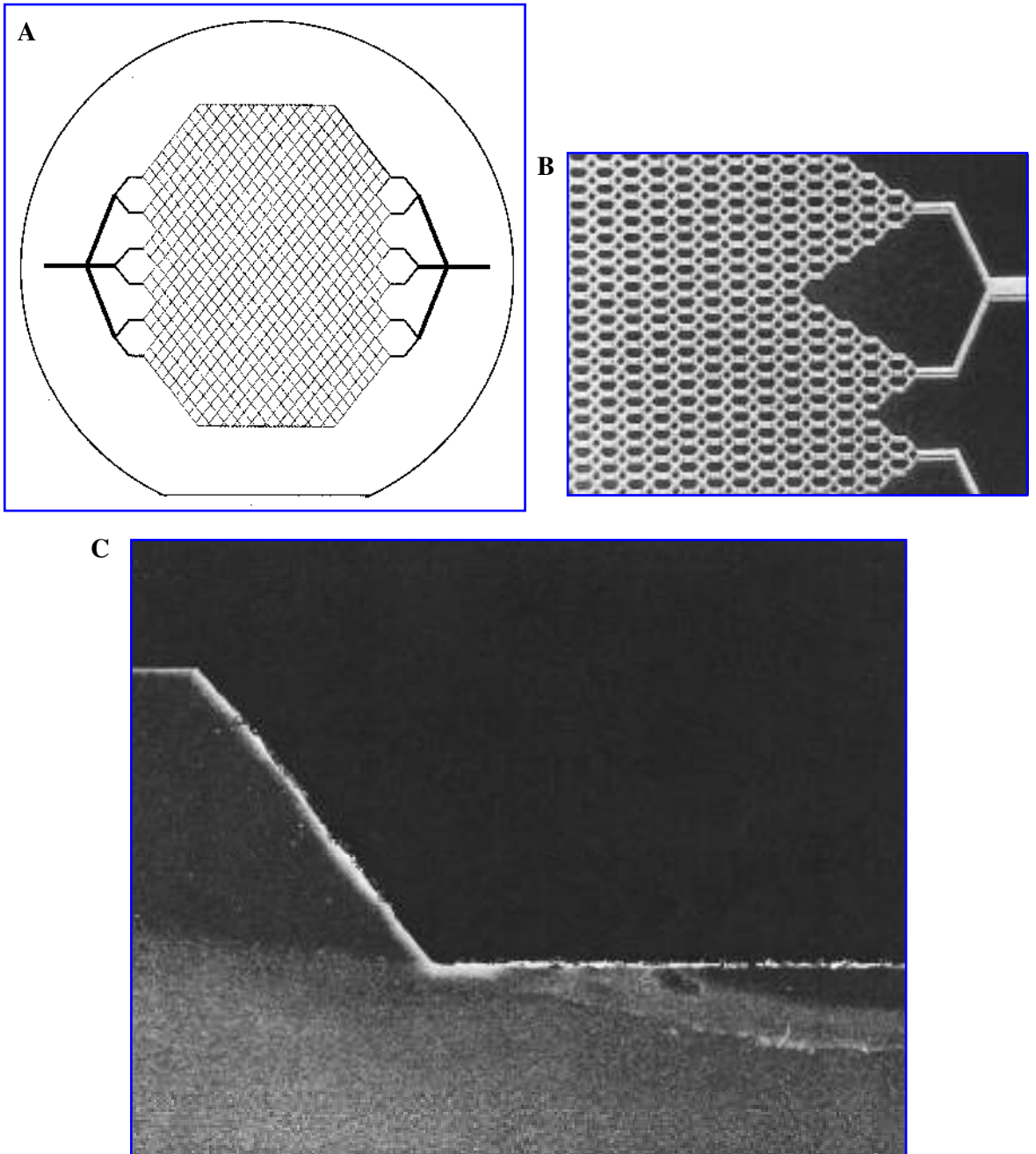


**FIG. 3.** (A) Vascular branching network pattern used for silicon and Pyrex wafer micromachining. (B) Optical micrograph of portion of capillary network etched into silicon wafer using the process shown in Fig. 1. (C) Scanning electron micrograph of anisotropic etching process used to form angled sidewall trenches (N. Gerrish and J. Ricker, Draper Laboratory).

#### *Growth and lifting of cells from unpatterned silicon and Pyrex wafers*

We studied the adhesion and growth of endothelial cells and hepatocytes on several different substrate surfaces. On all Pyrex wafers, coated or noncoated, the endothelial cells proliferated and grew to confluence within 4 days. These cells did not lift spontaneously, and, when scraped, did not lift as a single sheet. In addition, when the noncoated silicon wafers were seeded with endothelial cells, the cell sheet fragmented

upon lifting. On the other hand, endothelial cells seeded onto silicon surfaces coated with vitrogen ( $30 \mu\text{g/mL}$ ), Matrigel (1%), and gelatin ( $10 \text{ mg/mL}$ ) did lift with a cell scraper, and provided an intact monolayer sheet of endothelial cells. Upon microscopic observation, there were no significant differences in the effects of the three coatings on the detached cell sheets.

Hepatocytes also attached and spread well on all coated and noncoated Pyrex wafers, and did not lift spontaneously or in sheets when scraped after several days of growth. However, when seeded onto silicon wafers, they lifted spontaneously on all the noncoated and coated wafers (Fig. 4). The hepatocyte sheets lifted from the noncoated wafers after 3 days, but were very fragile and fragmented easily. The monolayers that lifted from the thin and thickly coated vitrogen substrates ( $30 \mu\text{g/mL}$  and  $3 \mu\text{g/mL}$ ) lifted after 4 days in culture to form an intact hepatocyte layer. Cells lifted from the Matrigel coated (1%) silicon wafers after 5 days in culture. There were no significant differences in appearance between the cell sheets lifted from the vitrogen and Matrigel-coated wafers.

Histological assessment of the detached cell monolayers of both hepatocytes and endothelial cells manifested promising results. Hematoxylin and eosin (H&E) staining of both showed that all cells were viable and that most were undergoing mitoses. The endothelial cells were observed to be primarily attenuated and to form a single-celled alignment (Fig. 5A). The monolayer of hepatocytes was of a spheroid configuration with eosinophilic flocculent cytoplasm and a large nucleus with a bright red nucleolus, similar to that seen in the native liver. Moreover, cellular attachments were less attenuated than the endothelial cells (Fig. 5B). Thus, these results are reminiscent of each of the cell types' specific functions. In biological systems, the endothelium functions as a barrier with a thin, smooth outer surface and as a transport channel and so it is understandable that these cells are observed here to be primarily attenuated and in a single-celled array. The hepatocytes have more of a tendency to form tissue and so we see less of a single-celled array and more of a rounded multi-layered array.

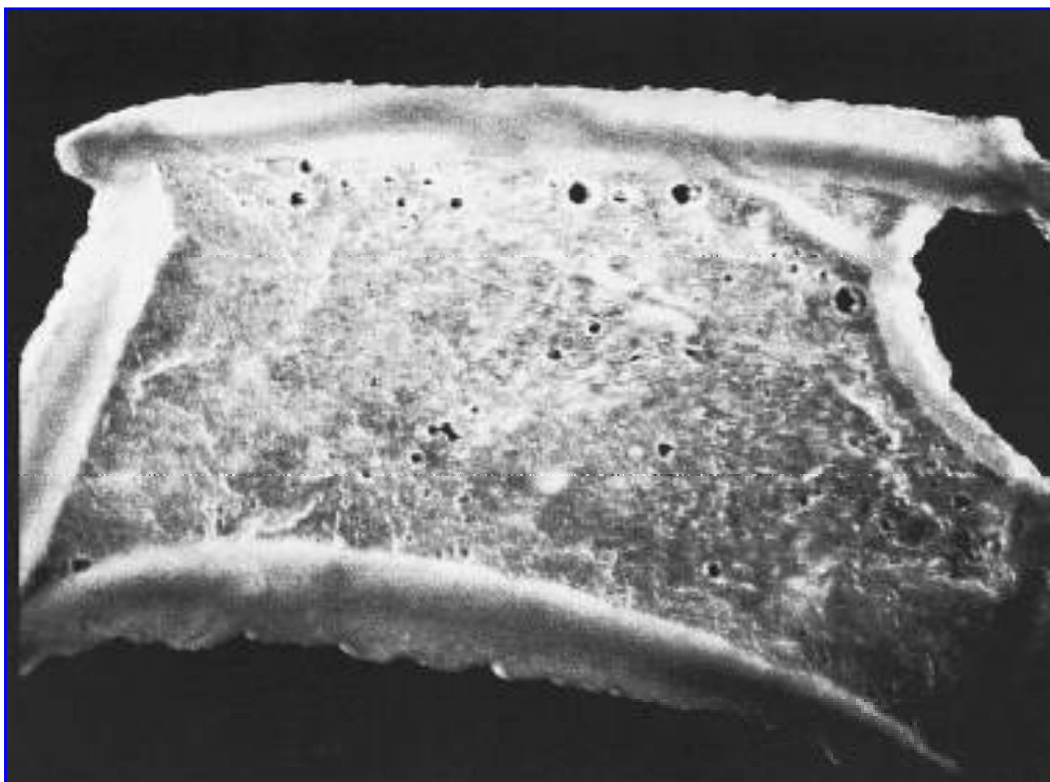


**FIG. 4.** Hepatocyte sheet lifted after 4 days in culture from a nonetched silicon surface coated with dilute vitrogen,  $30 \mu\text{g/mL}$  (Magnification:  $\times 8$ ).



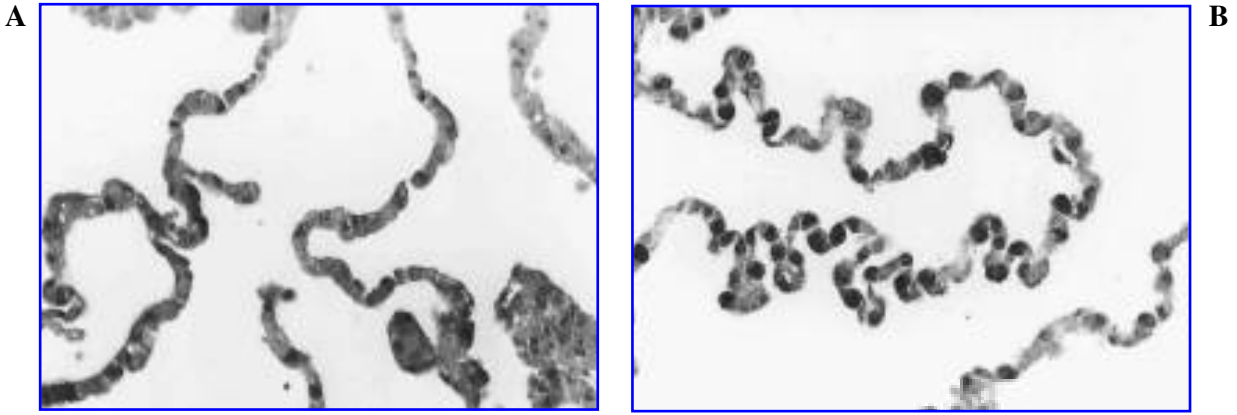


**FIG. 5.** (A) H&E staining for detached monolayers of hepatocytes. (B) H&E staining for detached monolayers of endothelial cells.

Values for albumin secretion into the hepatocyte culture medium at days 2, 3, 4, and 5 were  $165.96 \pm 29.87$ ,  $164.44 \pm 17.22$ ,  $154.33 \pm 18.46$ , and  $115.47 \pm 18.09$  ( $\mu\text{g/day}$ , Graph 1), respectively. Although there was a statistical significant difference between days 4 and 5, no significant differences were observed between days 2, 3, and 4 ( $p < 0.05$  by the paired  $t$ -test). Hence, this data shows the cells cultured on the silicon wafer were able to maintain a fairly constant rate of albumin production until day 4.

Moreover, through immunohistochemical staining of the detached hepatocyte monolayers, many cells were stained positive for albumin, indicating further that hepatocyte function was maintained while on the silicon wafers.

#### *Cell growth on etched surfaces of silicon and Pyrex wafers*

On all Pyrex and silicon-etched wafers, coated and noncoated, the endothelial cells proliferated and grew to confluence within 4 days inside and outside the channels. These cells did not lift spontaneously, but they did cover the walls of the channels. Hepatocytes also attached and spread on the etched Pyrex wafers, coated and noncoated, covering the walls of the channels. On the silicon wafers, the hepatocytes attached and spread, but did not lift spontaneously as with the nonetched wafers on the noncoated or vitrogen-coated ( $30 \mu\text{g/mL}$ ) wafers (Fig. 6).

#### *Implantation of hepatocyte sheet into the rat omentum*

H&E staining of hepatocyte sheets implanted into rat omentum demonstrated that all cells were viable and showed proliferation at 4 weeks and 3 months. The implanted hepatocyte monolayer sheets, when harvested, were over five cell layers thick in most areas (Fig. 7).

## DISCUSSION

This study demonstrates that silicon microfabrication technology can be used to form large sheets of living tissue. It also demonstrates the feasibility of etching ordered branching arrays of channels that allow living endothelial cells to line the luminal surface of the channels. In addition, we have shown that organized sheets of engineered hepatocyte tissue and endothelial tissue can be lifted from the surface of silicon or Pyrex wafers and can be folded into a compact three-dimensional configuration. We have then taken the hepatocyte sheets and placed them into rats on the highly vascular surface of the omentum. That structure has then been rolled into a three-dimensional cylinder as a model for an engineered vasculature. We show the formation of vascularized hepatic tissue as a permanent graft. These steps are preliminary first results

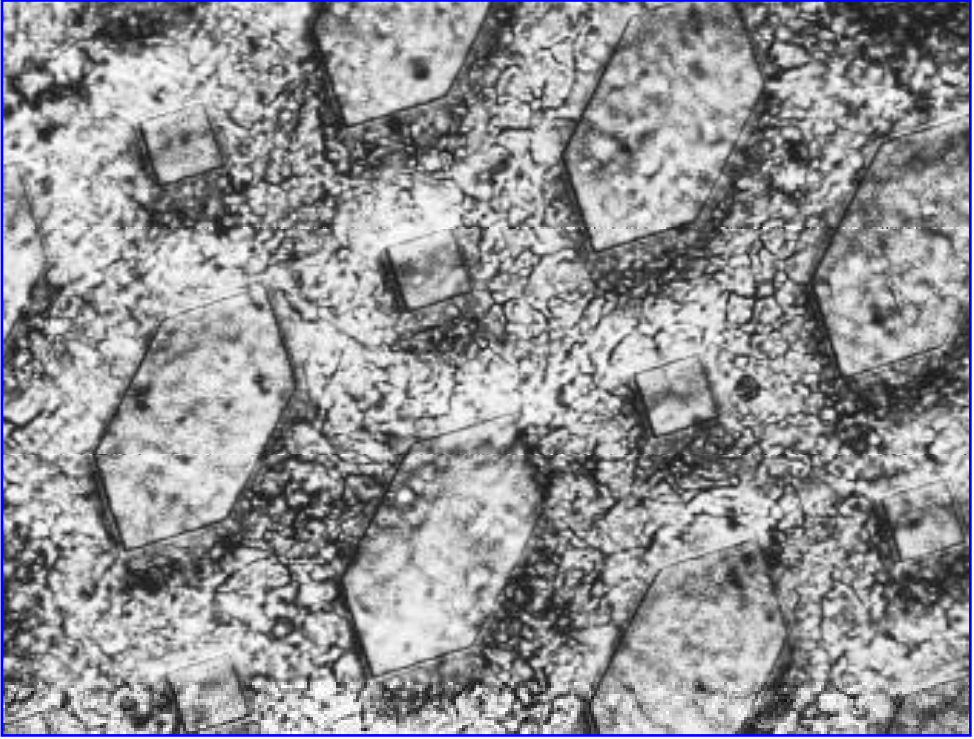


**FIG. 6.** Endothelial cells grown on vitrogen coated ( $30 \mu\text{g/mL}$ ) Pyrex wafers after 4 days in culture.

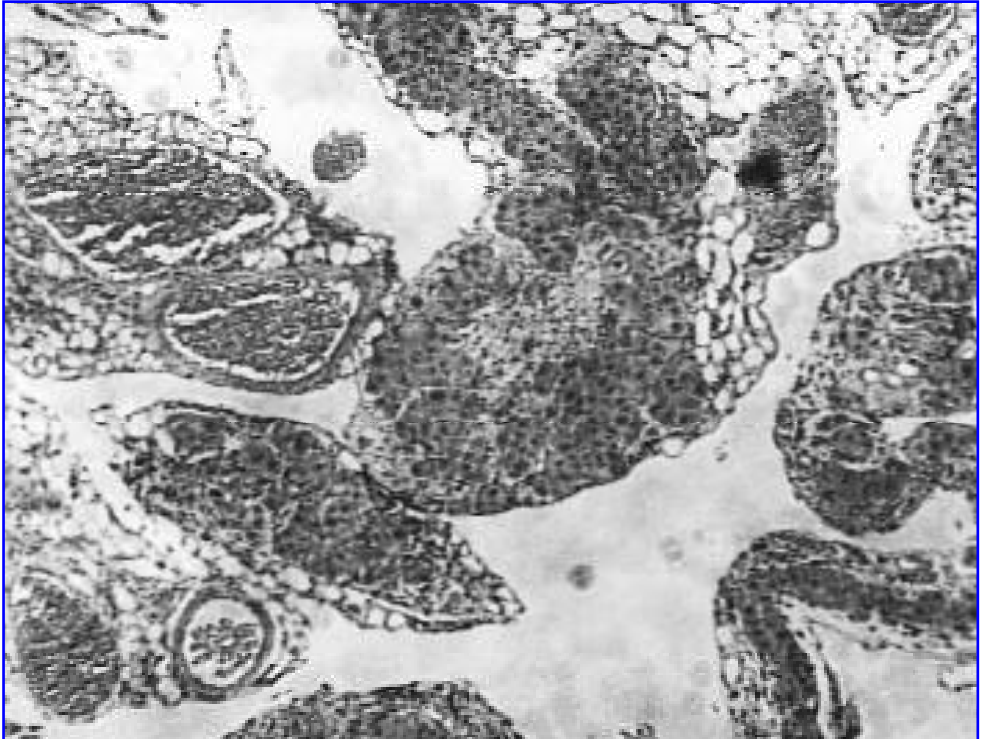


**FIG. 7.** H&E staining for hepatocyte sheets implanted into the rat omentum after 4 weeks. Over five cell layers are visible in most places.

toward a novel approach to the problem of generating complex, vascularized, thick tissues using the principles of tissue engineering.

The field of tissue engineering is now maturing as both a scientific and a clinical discipline. The concept of replacing living tissue with living tissue designed and then fabricated is less than 30 years old, although tumor cells were implanted into animals encased in a polymer membrane in 1933.<sup>31</sup> To date, all engineered tissue devices have been built as systems without a blood supply and have relied on vascularization from the host to provide permanent engraftment and mass transfer of oxygen and nutrients. These systems range from nonliving implants as forms of guided regeneration devices, to devices composed of living cells combined with some form of scaffolding.<sup>14</sup> This fundamental approach has shown broad utility in many different tissues of the body. However, an avascular approach to large vascular organs such as the liver, kidney, or heart has substantial shortcomings and has not been reliable in animal models. Because of this difficulty, we began to study possible approaches to provide a complete vascular system to the engineered structure before implantation. To date, three-dimensional printing has been used as a technology to provide an ordered array of branching channels to a polymer before cell seeding.<sup>17,32</sup>

This report is based on a novel concept that involves making a complete branching vascular circulation in two dimensions on the surface of silicon using the tools of microfabrication, and then lifting it from the silicon mold and folding or rolling it into a compact three-dimensional structure. The study demonstrates feasibility in several of the important components. Microfabrication technology has been used in important studies in cell and developmental biology to understand complex biologic signaling events occurring at the cell membrane-surface interface.<sup>23</sup> It has also been used in tissue engineering to guide cell behavior and the formation of small units of tissue.<sup>21</sup> To our knowledge, this is the first report of adapting the technology to make a coherent structure over a broad range of scale. The channels begin as a single channel with a diameter of 500  $\mu\text{m}$ , branch through four generations following a geometric scaling law that halves the channel width for each successive generation, form an array of capillary channels 10 microns in diameter, and then sequentially branch back to a single outflow vein. We have demonstrated that not only can we form the channels in silicon and Pyrex, but that living endothelial cells will line the channels. In other experiments, we have demonstrated that cells on surfaces of silicon and Pyrex will lay down matrix and form sheets of tissue of the cell type of origin, either hepatic or endothelial. We have also demonstrated the ability to peel these sheets from the surface and form three-dimensional units of tissue. In effect, the wafer of silicon or Pyrex has acted as a mold for the formation of tissue.

Microfabrication technology has been adapted to suit the needs of forming living tissue. Its potential power lies in its control of form over extremely small distances. The resolution is on the order of 0.1 microns from point to point. This level of precision adds new levels of control in our ability to design and guide new tissue formation. For instance, surfaces can be imprinted with submicron grooves or scallops, and corners can be made rounded, angled, or sharp with this same level of submicron precision. Geometric control at this scale can have a powerful impact on cell adhesion through mechanisms such as contact guidance.<sup>33</sup> The fundamental barrier to application has been that the technology for the purpose of tissue engineering was limited to very thin structures because designs were constrained to the surface of the silicon wafers. By using the wafer as a temporary mold and lifting the tissue from it, we have overcome this limitation and folded the tissue into three-dimensional space. It now seems feasible to consider lifting the channels formed from endothelial cells and combining them with layers of parenchymal tissue such as hepatocytes. After combining and folding into three dimensions, if flow can be initiated, vascularized tissue will have been fabricated. Those studies are currently underway. These preliminary studies can be expanded to studies that include specific surface chemistry alterations that can help with cell adhesion, cell proliferation, and matrix production. Advances in polymer chemistry can aid in the mechanical tasks of lifting and folding as well as the biologic tasks of adhesion and gene expression. Microfabrication appears to be a powerful new tool for the tissue engineer to not only understand the biology of tissue development but also to aid in the fabrication of large tissue and organ structures specifically designed for human therapy.

## ACKNOWLEDGMENTS

This work was supported by a generous grant from The Center For Innovative Minimally Invasive Therapy and the Department of Defense Grant #:DAMD17-99-2-9001. The authors gratefully acknowledge Ms. Miranda Kelly for her assistance in the preparation of the manuscript, and the students and technical staff of the Draper Laboratories who helped in the design and fabrication of the silicon and Pyrex wafers.

## REFERENCES

1. Vacanti, J.P., and Langer, R. Tissue engineering: the design and fabrication of living replacement devices for surgical reconstruction and transplantation. *Lancet* **354**, 32, 1999.
2. Langer, R., and Vacanti, J. Tissue engineering. *Science* **260**, 920, 1993.
3. Rennie, J. ed. Special report: The promise of tissue engineering. *Sci. Am.* **280**, 37, 1999.
4. Lysaght, M.J., Nguy, N.A.P., and Sullivan, K. An economic survey of the emerging tissue engineering industry. *Tiss. Eng.* **4**, 231, 1998.
5. Bell, E., Ehrlich, P., Buttle, D.J., and Nakatsuji, T. Living tissue formed in vitro and accepted as skin-equivalent of full thickness. *Science* **221**, 1052, 1981.
6. Burke, J.F., Yannas, I.V., Quimby, W.C., Bondoc, C.C., and Jung, W.K. Successful use of a physiologically acceptable artificial skin in the treatment of extensive burn injury. *Ann. Surg.* **194**, 413, 1981.
7. Compton, C., Gill, J., Bradford, D., Regauer, S., Gallico, G., and O'Connor, N. Skin regenerated from cultured epithelial autografts on full-thickness burn wounds from 6 days to 5 years after grafting. *Lab. Invest.* **60**, 600, 1989.
8. Parenteau, N., Nolte, C., Bilbo, P., Rosenburg, M., Wilkins, L., Johnson, E., Watson, S., Mason, V., and Bell, E. Epidermis generated in vitro: practical considerations and applications. *J. Cell. Biochem.* **45**, 24, 1991.
9. Parenteau, N., Sabolinski, M., Prosky, S., Nolte, C., Oleson, M., and Kriwet, K. Biological and physical factors in influencing the successful engraftment of a cultured human skin substitute. *Biotechnol. Bioeng.* **52**, 3, 1996.
10. Purdue, G.F., Hunt, J.L., et al. A multicenter clinical trial of a biosynthetic skin replacement, Dermagraft-TC, compared with cryopreserved human cadaver skin for temporary coverage of excised burn wounds. *J. Burn Care Rehab.* **18**, 52, 1997.
11. Hansbrough, J.F., and Franco, E.S. Skin replacements. *Clin. Plastic Surg.* **25**, 407, 1998.
12. Vacanti, C.A., Cima, L.G., Ratkowski, D., Upton, J., and Vacanti, J.P. Tissue engineered growth of new cartilage in the shape of a human ear using synthetic polymers seeded with chondrocytes. In: Cima LG, Ron ES, eds. *Tissue-inducing biomaterials*, Materials Research Society Symposium Proceedings, Pittsburgh: Materials Research Society **252**, 367, 1992.
13. Isogai, N., Landis, W., Kim, T.H., Gerstenfeld, L.C., Upton, J., and Vacanti, J.P. Tissue engineering of a phalangeal joint for application in reconstructive hand surgery. *J. Bone Joint Surg. Am.* **81**, 306, 1999.
14. Lanza, R., Langer, R., Chick, W. eds. *Principles of Tissue Engineering*. Austin, TX: Academic Press, 1997.
15. Pedersen, R. Embryonic stem cells for medicine. *Sci. Am.* **44**, 68, 1999.
16. Thomson, J.A., Itskovitz-Eldor, J., Shapiro, S.S., et al. Embryonic stem cell lines derived from human blastocysts. *Science* **282**, 1145, 1998.
17. Griffith, L.G., Wu, B., Cima, M.J., Powers, M.J., Chaignaud, B., and Vacanti, J.P. In vitro organogenesis of liver tissue. *Ann. NY Acad. Sci.* **831**, 382, 1997.
18. Langer, R., and Vacanti, J.P. Tissue engineering: the challenges ahead. *Sci. Am.* **280**, 62, 1999.
19. McWhorter, P.J., Frazier, A.B., and Rai-Choudhury, P. Micromachining and trends for the twenty-first century. In: P. Rai-Choudhury, ed. *Handbook of Microlithography, Micromachining and Microfabrication*, Bellingham, WA: SPIE Press, 1997.
20. Kourepenis, A., Borenstein, J., Connelly, J., Elliott, R., Ward, P., and Weinberg, M. Performance of MEMS inertial sensors. *Proc. AIAA GN&C Conference*, Boston, MA, 1998.
21. Griffith, L., Powers, M., and Tannenbaum, S. Microfabricated structures for control of 3D co-cultures of liver cells. *Ann. Biomed. Eng.* **26**, 1998.
22. Folch, A., and Toner, M. Cellular micropatterns on biocompatible materials. *Biotechnology Progr.* **14**, 388, 1998.
23. Kane, R.S., Takayama, S., Ostuni, E., Ingber, D.E., and Whitesides, G.M. Patterning proteins and cells using soft lithography. *Biomaterials* **20**, 2363, 1999.
24. Ayon, A.A., Chen, K.S., Lohner, K.A., Spearing, S.M., Sawin, H.H., and Schmidt, M.A. Deep reactive ion etching of silicon. *Mat. Res. Soc. Symp. Proc.* **546**, 51, 1999.

25. Kendall, D.L., Malloy, K.J., and Fleddermann, C.B. Critical technologies for the micromachining of silicon. In: K.T. Faber and K.J. Malloy, eds. *Semiconductors and Metals*. New York: Academic Press, 1992.
26. Aiken, J., Cima, L., Schloo, B., et al. Studies in rat liver perfusion for optimal harvest of hepatocytes. *J. Pediatr. Surg.* **25**, 140, 1990.
27. Seglen, P.O. Preparation of isolated rat liver cells. *Methods Cell Biol.* **13**, 29, 1976.
28. Niklason, L.E., Gao, J., Abbott, W.M., et al. Functional arteries grown in vivo. *Science* **284**, 489, 1999.
29. Schwere, B., Bach, M., and Bernheimer, H. ELISA for determination of albumin in the nanogram range: assay in cerebrospinal fluid and comparison with radial immunodiffusion. *Clin. Chem. Acta* **163**, 237, 1987.
30. Peterson, J.E. Effects of the pyrrolizidine alkaloid lasiocarpine-N-oxide on nuclear and cell division in the liver of rats. *J. Pathol. Bacteriol.* **89**, 153, 1965.
31. Bisceglie, V. Uber die antineoplastische immunitat; heterologe Einpflanzung von Tumoren in Huhner-embryonen. *Ztschr f Krebsforsch* **40**, 122, 1933.
32. Kim, S.S., Utsunomiya, H., Koski, J.A., Wu, B.M., Cima, M.J., Sohn, J., Mukai, K., Griffith, L.G., and Vacanti, J.P. Survival and function of hepatocytes on a novel three dimensional synthetic biodegradable polymer scaffold with an intrinsic network of channels. *Ann. Surg.* **228**, 8, 1998.
33. Den Braber, E.T., de Ruijter, J.E., Ginsel, L.A., von Recum, A.F., and Jansen, J.A. Orientation of ECM protein deposition, fibroblast cytoskeleton, and attachment complex components on silicon microgrooved surfaces. *J. Biomed. Mater. Res.* **40**, 291, 1998.

Address correspondence to:

*Joseph P. Vacanti, M.D.*

*John Homans Professor of Surgery*

*Harvard Medical School and Massachusetts General Hospital*

*55 Fruit Street, Warren 1157*

*Boston, MA 02114*

*E-mail: jvacanti@partners.org*